Review

Israel Journal of Chemistry

DOI: 10.1002/ijch.201800172

Tracking CO Release in Cells via the Luminescence of Donor Molecules and/or their By-Products

Tatiana Soboleva[a] and Lisa M. Berreau*[a]

Abstract: Carbon monoxide (CO) is a bioactive signalling molecule that is produced endogenously via the breakdown of heme. Beneficial health effects associated with the delivery of CO gas have spurred the development of CO-releasing molecules (CORMs) that can be used to provide specific amounts of the gas. In addition to their potential use as therapeutics, CORMs are needed to provide insight into the biological targets of CO. In this regard, light-activated CO-releasing molecules (photoCORMs), are valuable for examining the effects of localized CO release. Herein we examine luminescent CORMs and photoCORMs that have been reported for tracking CO delivery in cells. A variety of motifs are available that exhibit differing luminescence properties and cover a wide range of wavelengths. Trackable CO donors have been successfully applied to targeting CO delivery to mitochondria, thus demonstrating the feasibility of using such molecules in detailed investigations of the biological roles of CO.

Keywords: luminescence · fluorescence · carbon monoxide · carbonyl ligands · photochemistry

1. Introduction

Bioimaging methods provide a powerful non-invasive approach toward interrogating cellular processes. In this context, numerous luminescent molecules have been developed as tools to gain insight into the cellular environment.[1] In this critical review, we summarize recently developed luminescent molecules capable of tracking the cellular delivery of carbon monoxide (CO), a gaseous signalling molecule that is formed in humans via the enzyme-catalyzed degradation of heme.[2] Despite its reputation as a toxic gas, CO is now recognized as a biologically important signalling molecule, producing effects *in vivo* primarily through interactions with low-valent metal centers.[3] The beneficial health effects identified with the introduction of exogenous CO gas include anti-inflammatory and vasodialation effects.[4] Tracking the delivery location of CO is essential toward understanding its localized effects on human health.[5]

To avoid the challenges associated with the delivery of CO gas, small molecules that release CO under physiological conditions, termed carbon monoxide-releasing molecules (CORMs), are now routinely used to probe the biological effects of this signalling molecule.[6] The most widely used CORMs to date are metal carbonyl compounds that lack features which would enable spatiotemporal tracking of their CO release in cellular environments.[7] These include the Ru(II) carbonyl derivatives $[RuCl_2(CO)_3]_2$ (CORM-2)[8] and $[Ru(CO)_3Cl(glycinate)]$ (CORM-3),[9] and the Mn(I) derivative $Mn(CO)_4(S_2CNMe(CH_2CO_2H))$ (CORM-401),[10] all of which spontaneously release CO via ligand exchange in aqueous environments (Figure 1). The CO release products of these compounds, termed inactivated CORMs or iCORMs, are not well defined and also cannot be tracked in biological environments. Over the past ~10 years several additional types of metal carbonyl CORMs have been developed, including complexes that enable more control over the site of CO delivery. These include CORMs that can be triggered for CO release using stimuli such as light (photoCORMs), enzyme activity (ETCORMs), or magnetic heating.[11] For targeting purposes and/or to limit toxicity of the iCORM following CO release, metal carbonyl CORMs have also been incorporated

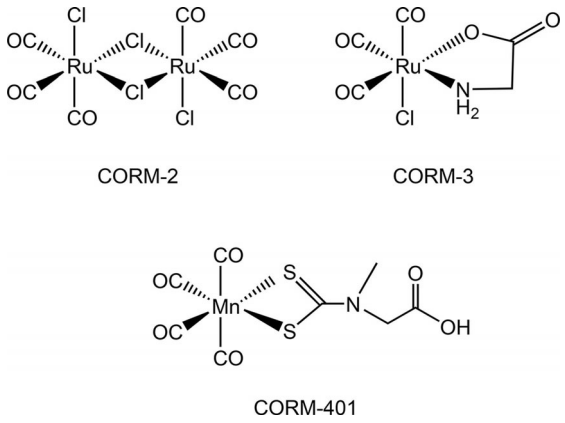

Figure 1. Spontaneous metal carbonyl-based CO-releasing molecules.

[a] T. Soboleva, L. M. Berreau
Department of Chemistry & Biochemistry
Utah State University
0300 Old Main Hill, Logan, Utah 84322-0300, United States
E-mail: tatiana.soboleva@aggiemail.usu.edu
lisa.berreau@usu.edu

© 2019 Wiley-VCH Verlag GmbH & Co. KGaA, Weinheim

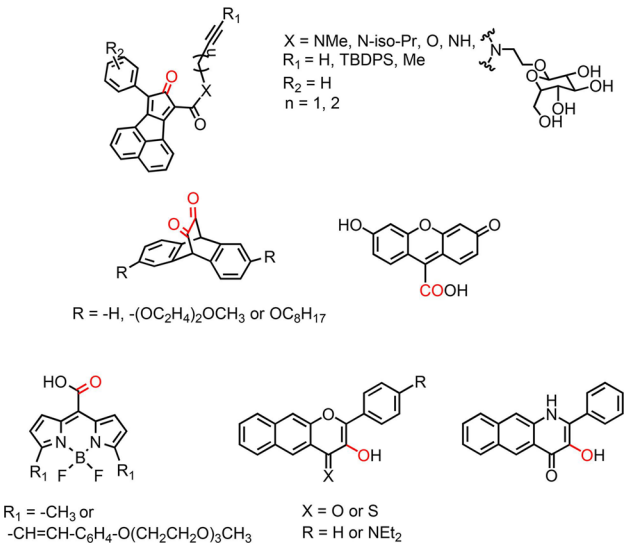

Figure 2. Frameworks of non-metal CORMs (top) and photoCORMs (middle and bottom). The C–O unit highlighted in red is the source of CO.

into biocompatible structures such as proteins, polymers, dendrimers, and metal organic frameworks.[12] Despite these advances, the majority of metal carbonyl CORMs reported to date cannot be tracked in terms of their cellular uptake and/or CO release process.

Several examples of metal-free CORMs and photoCORMs have also been recently reported. Wang and co-workers have designed molecules which undergo either inter- or intramolecular inverse electron demand Diels-Alder (DA_{inv}) reactions to form norbornadien-7-ones. These structures subsequently undergo a cheletropic reaction to spontaneously release CO under mild conditions (Figure 2(top)).[13] Other scaffolds have been used to develop metal-free photoCORMs, including cyclic α-diketones, a xanthene carboxylic acid, mesocarboxy BODIPYs, and 3-hydroxyflavone and 3-hydroxyquinolone motifs (Figure 2(middle and bottom)).[14]

CORMs and photoCORMs that can be tracked via luminescence offer the advantage of providing insight into cellular uptake and distribution, as well as the CO release process in living cells.[1,15] This is an important and timely issue as the reactivity of CO with known and yet unidentified cellular targets may be impacted by the proximity of CO delivery. In this review we critically examine the examples reported to date of luminescent metal carbonyl and metal-free CORMs, photoCORMs, and iCORMs. We discuss the bioapplicability of these compounds in terms of cellular uptake of the CORMs and/or evidence of their CO release. We also note the cellular toxicity of each luminescent CORM, if reported, as well as their iCORMs. Additionally, we describe an application of using a trackable CO-releasing molecule to target CO delivery to mitochondria. These studies provide insight into how cytosolic versus mitochondrial-localized CO release influences O_2 consumption by the heme-containing cytochrome c oxidase in the mitochondrial electron transport chain.

2. Luminescent Metal Carbonyl CO-Releasing Molecules and their By-Products

The development of luminescent metal carbonyl CO-releasing molecules has progressed quickly over the past few years. The general formula of such complexes is $[MX(CO)_3(\alpha\text{-diimine})]$ where M = Re(I) or Mn(I), the axial ligand X is an anion or neutral monodentate ligand, and the α-diimine is a bidentate ligand such as bipyridine (bpy), 1,10-phenanthroline (phen) or 2-(2-pyridyl)-benzothiazole (pbt). The emission properties of these complexes are associated with luminescence from a ^{3}MLCT excited state or from the axial X or α-diimine ligands, or from released aromatic ligands.[16] The specific combination of ligands enable the complex to exhibit trackable luminescence, turn-off/turn-on properties upon CO-release, or to exhibit emissive properties both before and after CO release (two-tone). All of the luminescent $[MX(CO)_3(\alpha\text{-diimine})]$ derivatives described herein function as photoCORMs. Generally these complexes have not been examined in detail regarding the photoreaction (e.g., quantum yield) leading to CO release. In many examples the products of the CO release reaction have also not been fully characterized. Despite these limitations, the complexes reported offer novel approaches for tracking CO delivery.

Lisa M. Berreau received her B.S. in chemistry from Minnesota State University, Mankato in 1990 and her Ph.D. in inorganic chemistry from Iowa State University in 1994 (w/L. Keith Woo). Following an NIH postdoctoral fellowship at the University of Minnesota working in the laboratory of William B. Tolman she joined the faculty at Utah State University in 1998. She is currently a Professor of Chemistry and Associate Vice President for Research at Utah State University.

Tatiana Soboleva received her B.S. in biochemistry from Minnesota State University, Mankato in 2016. She is currently a Presidential Doctoral Research Fellow and American Heart Association Predoctoral Fellow at Utah State University, working on her Ph.D. in organic chemistry under the direction of Professor Lisa M. Berreau. Tatiana is exploring the chemical properties and biological effects of visible light-induced CO-releasing molecules based on a 3-hydroxyflavone motif.

© 2019 Wiley-VCH Verlag GmbH & Co. KGaA, Weinheim

2.1 Trackable Re(I) and Mn(I) Metal Carbonyl PhotoCORMs

One approach for tracking intracellular CO delivery is to monitor the luminescence of a photoCORM prior to CO release. This method has been explored by Mascharak and co-workers using Re(I)-based photoCORMs.[17] Each Re(I) complex shown in Figure 3 exhibits an emission in the range of 500–620 nm. Complexes 1–4 release CO in the presence of low-power UV light (5 mW/cm^2; centered at 302 nm), with the number of CO molecules released (1–3) depending on the monodentate ligand in the axial position. Complexes 1–3 were studied in terms of cellular uptake and intracellular distribution within human metastatic breast adenocarcinoma cells (MDA-MB-231) prior to CO release using confocal microscopy (Figure 4).[17] All showed cytosolic distribution except $[Re(CO)_3(PPh_3)(phen)]O_3SCF_3$ (2, Figure 4) which was also identified to accumulate in nuclei.[17a] No cytotoxicity data were reported for 1–3. Complex 4, $[Re(CO)_3(phen)(pyAl)]O_3SCF_3$ (where pyAl = pyridine-4-carboxaldehyde), which was grafted on to a biocompatible carboxymethyl chitosan (CMC) matrix, was found to be taken up by MDA-MB-231 breast cancer cells and HT-29 colon cancer cells as evidenced by intracellular emission at 550 nm.[17b] In the absence of illumination to induce CO release, complex 4 shows no apparent cellular toxicity. However, a dose dependent eradication of HT-29 cells was observed upon UV light-induced CO release.[17b]

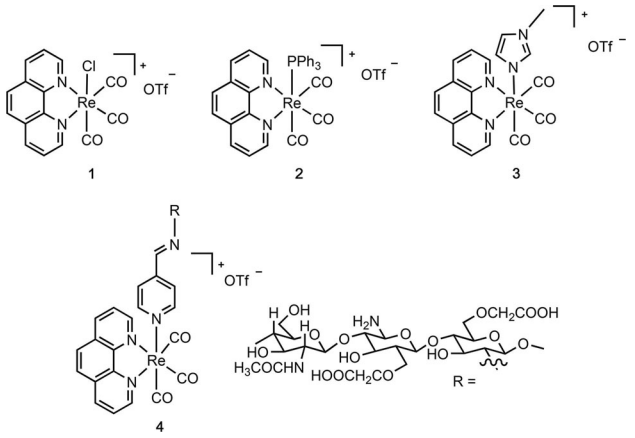

Figure 3. Trackable Re(I) photoCORMs.

The first examples of luminescent Mn(I) photoCORMs were recently reported by Mascharak and co-workers.[18,19] Typically, photoCORMs containing the $[Mn(I)(CO)_3]$ unit are not luminescent even with coordinated emissive ligands due the electron withdrawing effect of the CO ligands.[20] A high percentage of the luminescence of the coordinated ligands in $[Mn(Imdansyl)(CO)_3(phen)]O_3SCF_3$ (**5**, $\lambda_{em} = 600$ nm) and $[Mn(Pipdansyl)(CO)_3(phen)]O_3SCF_3$ (**6**, $\lambda_{em} = 530$ nm) (Figure 5(top)) is retained because of the separation of the metal center from the axial ligand via a linker. Internalization of the compounds in HT-29 colon cancer cells was determined using confocal microscopy (**5**, Figure 5(bottom)). Illumination of CH_3CN solutions of **5** and **6** with low intensity broadband visible light results in loss of all three CO ligands, release of the dansyl ligands, and the formation of Mn(II) by-products. As the luminescence of the product mixtures are similar to those exhibited by **5** and **6**, studies of the intracellular CO release reactions were not pursued. As the photoCORMs in

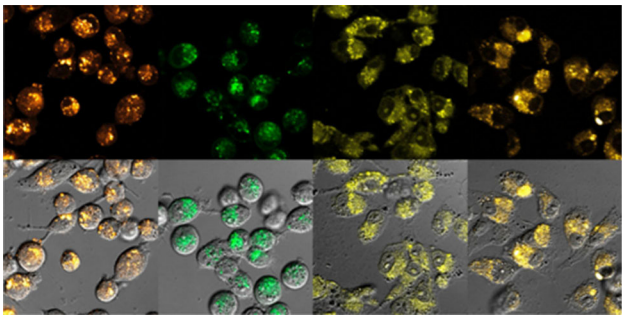

Figure 4. (top) Confocal microscopy fluorescence images of (left to right) **1**, $[Re(CO)_3(CH_3CN)(phen)]O_3SCF_3$ (structure not shown), **2** and **3**. (bottom) Overlaid fluorescence and bright field images of MDA-MB-231 cells with complexes. Reprinted (adapted) with permission from (I. Chakraborty, J. Jimenez, W. M. C. Sameera, M. Kato, P. K. Mascharak, *Inorg. Chem.* **2017**, *56*, 2863–2873). Copyright (2017) American Chemical Society.

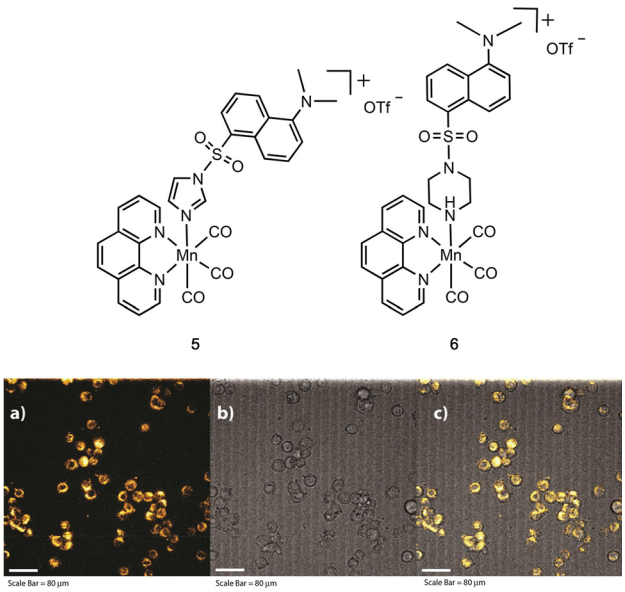

Figure 5. Top: $[Mn(Imdansyl)(CO)_3(phen)]O_3SCF_3$ (**5**) and $[Mn(Pipdansyl)(CO)_3(phen)]O_3SCF_3$ (**6**). Bottom: Fluorescence microscope images of **5** in HT-29 colon cancer cells: a) fluorescence image, b) bright field image, and c) merged image. Reprinted (adapted) with permission from (J. Jimenez, I. Chakraborty, A. Dominguez, J. Martinez-Gonzalez, W. M. C. Sameera, P. K. Mascharak, *Inorg. Chem.* **2018**, *57*, 1766–1773). Copyright (2018) American Chemical Society.

© 2019 Wiley-VCH Verlag GmbH & Co. KGaA, Weinheim

this category are not differentiated from those of the iCORMs following CO release in terms of their luminescence properties, these compounds offer limited insight into the CO delivery process in cellular environments.

2.2 Turn-Off Re(I) PhotoCORMs

A more insightful approach to assess CO delivery is via the use of photoCORMs that exhibit trackable luminescence with turn-off behaviour upon CO release. Examples of Re(I) compounds of this type have been recently developed.[21,22] The first example was reported in the context of designing metal carbonyl-loaded mesoporous silica nanoparticles for CO delivery.[21] $[Re(CO)_3(pbt)(PPh_3)]O_3SCF_3$ (**7**, Figure 6) exhibits a strong ^{3}MLCT luminescence at 605 nm upon excitation at 345 nm. Upon illumination of a CH_3CN solution of **7** with low power UV light one equivalent of CO is released and a decrease of the ^{3}MLCT luminescence intensity is observed. Al-MCM-41 mesoporous silica nanoparticles loaded with the complex, {Re-CO}@Al-MCM-41, also exhibit trackable and turn-off luminescence behaviour in PBS solution.[21] Uptake of the {Re-CO}@Al-MCM-41 nanoparticles by MDA-MB-231 breast cancer cells was confirmed via confocal microscopy which revealed the orange-red luminescence (λ_{em} = 585 nm) of the {Re-CO}@Al-MCM-41 nanoparticles in the cellular matrix (Figure 7). Upon exposure of the cells to 30 minutes of UV light (305 nm; power: 5 mW/cm^2) a decrease of the orange-red luminescence was observed, which is indicative of CO release. The luminescence properties of **7** thus allow for tracking of both the localization of the compound in cells and the CO release reaction. The water soluble $[Re(CO)_3(pbt)(PTA)]O_3SCF_3$ (**8**, PTA = 1,3,5-triaza-7-phosphaadamantane) and $[Re(CO)_3(phen)(PTA)]O_3SCF_3$ (**9**) (Figure 8) exhibit similar CO release and turn-off emissive properties (λ_{em} ~ 550 nm), with the former having also been evaluated in MDA-MB-231 cells.[22]

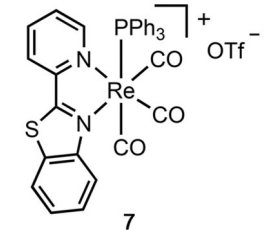

7

Incorporated in the pores of Al-MCM-41 mesoporous silica nanoparticles.

Figure 6. Trackable turn-off photoCORM.

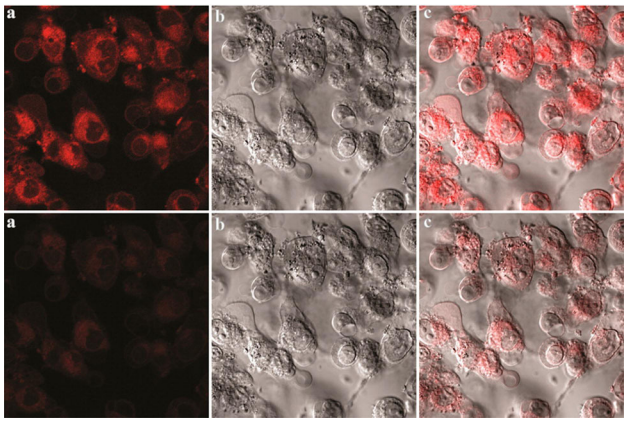

Figure 7. Confocal microscopy images of MDA-MB-231 breast cancer cells after incubation with {Re-CO}@Al-MCM-41 mesoporous silica nanoparticles for 3 h (λ_{ex} = 302 nm; λ_{em} ~ 600 nm). Upper panel: a) fluorescence image, b) bright field image, c) merged image; Lower panel: a) fluorescence dimmed after 30 min of UV illumination, b) bright field image, and c) merged image. Reprinted with permission from (I. Chakraborty, S. J. Carrington, J. Hauser, S. R. J. Oliver, P. K. Mascharak, *Chem. Mater.* **2015**, *27*, 8387–8397). Copyright (2015) American Chemical Society.

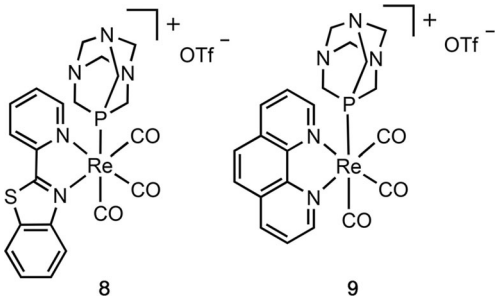

8 9

Figure 8. Water soluble luminescent turn-off CO-releasing molecules.

Despite their potential for use as trackable photoCORMs for CO release in cellular environments, the luminescent Re(I)-containing complexes and nanoparticles described above have some limitations. For example, all are triggered for CO release by UV-B light, which impedes deep tissue penetration and is potentially problematic for use in mammalian systems due to the potential for mutagenesis.

2.3 Turn-On Mn(I)-Based CO-Releasing Molecules

Several Mn(I) complexes containing a chelate fluorescent ligand and the $[Mn(I)(CO)_3]$ unit have been shown to act as turn-on photoCORMs for tracking CO release. Mascharak and co-workers reported that the Mn(I) photoCORMs **10** and **11** (Figure 9) exhibit turn-on luminescence behaviour upon visible light-induced CO release.[22,23] The appearance of luminescence in these complexes is associated with the oxidation of Mn(I) to Mn(II) and the release of the bidentate 2-(2-pyridyl)-benzothiazole (pbt) ligand, which exhibits a blue emission (λ_{em} = 400 nm) as a free organic molecule. This

© 2019 Wiley-VCH Verlag GmbH & Co. KGaA, Weinheim

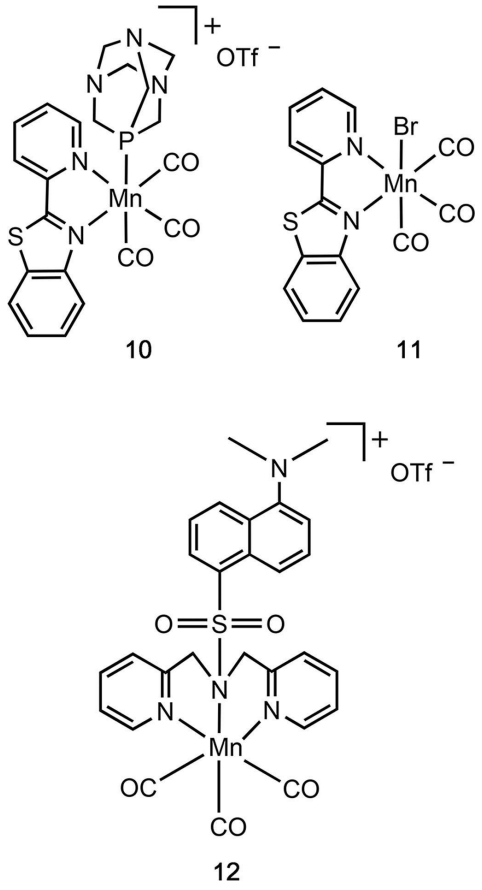

Figure 9. Turn-on Mn(I) photoCORMs.

change also corresponds to the release of all three CO ligands. To date, the feasibility of **10** as a turn-on photoCORM in cells has not been reported.[22] Toxicity studies show that **10** does exhibit CO-induced dose-dependent eradication of MDA-MB-231 cells (~50% at 100 μM). Control experiments involving Mn(II) salts and the free pbt ligand showed only a minor reduction in cell viability, indicating that the release of CO from **10** is the primary reason for the observed enhanced cytotoxicity.

The second Mn(I) turn-on photoCORM reported from the Mascharak lab is [$MnBr(CO)_3$(pbt)] (**11**, Figure 9).[23] Its luminescence turn-on is also associated with the dissociation of the pbt ligand upon visible-light induced CO release (λ_{ill} = 405 nm). This complex was visualized in MDA-MB-231 cells, showing a 20-fold enhancement of the blue fluorescent signal upon CO release.

Schiller and co-workers have described the turn-on fluorescence properties of a Mn(I)$(CO)_3$ complex containing a dansyl-appended dipyridyl amine ligand (**12**, Figure 9) in the context of a molecular logic gate.[20] The input of either visible light (405 nm) or H_2O_2 results in the formation of CO, light (fluorescent emission at ~514 nm), and a dipyridyl amine-coordinated Mn(II) product (as proposed based on EPR and ^{1}H NMR investigations). Confocal microscopy studies performed using HCT116 colon cancer cells showed the turn-on associated with CO release (Figure 10). Cell viability studies performed in two other cells lines (HepaRG (progenitor cells) and LX-2 (stellate cells)) indicated mild cytotoxicity (EC_{50} values 73 ± 5.7 μM and 114 ± 4.6 μM, respectively). Under dark and light conditions, complex **12** exhibits enhanced toxicity in cancer cells (~10–30 μM).

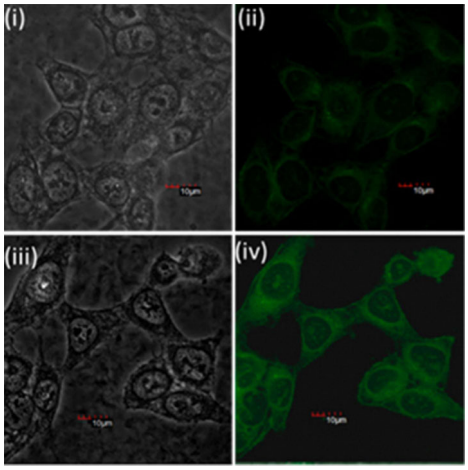

Figure 10. Confocal microscopy images of HCT116 colon cancer cells incubated with **12** (10 μM) for 30 min at 37 °C (λ_{ex} = 365 nm; λ_{em} = 510 nm): (i,iii) bright field images, (ii) no light exposure, (iv) fluorescence image following three 10 s pulses of low-powered LED light (405 nm). Reprinted (adapted) with permission from (U. Reddy G., J. Althelm, P. Hoffmann, N. Taye, S. Gläser, H. Görls, S. L. Hopkins, W. Plass, U. Neugebauer, S. Bonnet, A. Schiller, *J. Am. Chem. Soc.* **2017**, *139*, 4991–4994). Copyright (2017) American Chemical Society.

Turn-on photoCORMs offer the possibility of detecting the CO release step but do not allow for tracking of the photoCORM uptake or localization of the CO-releasing molecule prior to CO delivery. This limits their utility to being similar to detecting CO using a fluorescent sensor such as COP-1.[24] An additional concern for use of these compounds in biological studies is the release of multiple by-products, including potentially bioactive transition metal ions.

2.4 Emissive Metal Carbonyl PhotoCORMs with Unique Fluorescence Signals Pre- and Post CO Release (Two-Tone CORMs)

The turn-off and turn-on complexes described above enable visualization of CO delivery via one of two time points – either prior to or following CO release. Luminescent photoCORMs that can be identified both pre- and post-CO release offer added visualization capability. Two metal carbonyl complexes of this type have been reported to date. The water soluble Re(I) photoCORM [$Re(bpy)(CO)_3$(thp)]O_3SCF_3 (**13**, Figure 11; bpy = 2,2'-bipyridine, thp = tris(hydroxymethyl)

© 2019 Wiley-VCH Verlag GmbH & Co. KGaA, Weinheim

Israel Journal of Chemistry

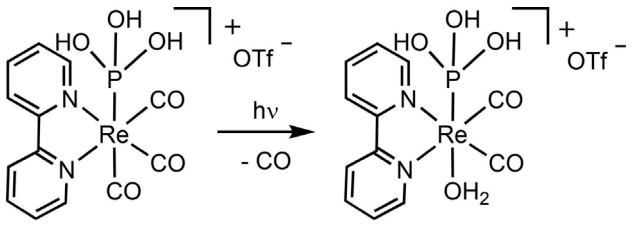

13 14

Figure 11. Visible light-induced CO release from **13** to produce **14**. Both complexes are luminescent and trackable in cells.

phosphine) reported by Ford and co-workers is strongly luminescent in aqueous solutions, with an emission band centered at 515 nm ($\lambda_{ex}=365$ nm; $\Phi_{em}=0.18$).[25] This band is assigned to the luminescence from the ^{3}MLCT excited state.[26] Illumination of **13** with visible light (405 nm) results in the loss of one CO ligand and the formation of **14**, which is also strongly luminescent, with an emission maximum at 585 nm ($\lambda_{ex}=405$ nm; $\Phi_{em}=0.15$). Confocal microscopy studies have shown that **13** accumulates in the cytoplasm of human prostatic carcinoma cells (PPC-1). Exposure of the cells to 405 nm light results in a decrease in emission intensity in the 465–495 nm window and enhanced emission at longer wavelengths (Figure 12). This change correlates with the light-induced CO delivery. The toxicity of **13** and **14** were examined in PPC-1 cells over a short time period (~2 h). Concentrations

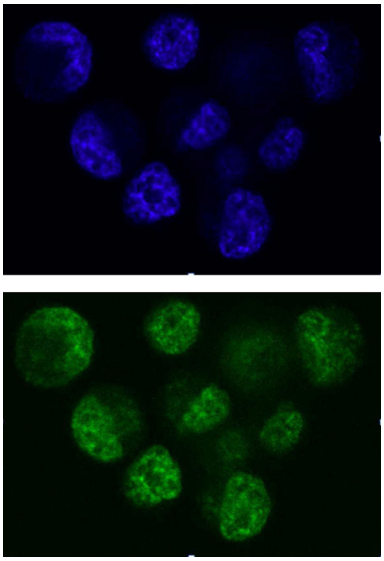

Figure 12. Confocal microscopy images of PPC-1 cells incubated with **13** (50 μM) for 60 min. The top image was collected with minimal exposure to the 405 nm excitation source ($\lambda_{em}=465$–495 nm). The bottom image was collected after exposure of the cells to the 405 nm light for 15 min. Reprinted (adapted) with permission from (A. E. Pierri, A. Pallaro, G. Wu, P. C. Ford, *J. Am. Chem. Soc.* **2012**, *134*, 18197–18200). Copyright (2012) American Chemical Society.

up to 100 μM produced no immediate adverse effect (>88% cell viability).

Inspired by this work, Mascharak and co-workers synthesized and characterized the Re(I)-based photoCORM $[Re(H_2O)(CO)_3(pbt)]O_3SCF_3$ (**15**, Figure 13).[27] This complex releases CO upon exposure to low-power UV illumination. Photolysis is accompanied by a blue-shift in luminescence from ~605 nm to ~400 nm upon CO release. Studies performed using human MDA-MB-231 breast cancer cells and a fluorescence microscope with Texas red ($\lambda_{em}\geq 604$ nm) and DAPI filters ($\lambda_{em}\geq 390$ nm) showed that upon excitation at 350 nm the longer wavelength emission diminishes while the emission at ~400 nm is enhanced. Similar to the turn-on probes noted above, the change in emission is associated with the loss of the pbt ligand from the Re(I) center. Complex **15** and the CO release products (each at 50 μM) were shown via MTT assay to produce minimal effects on cell viability under dark conditions. The reduction in cellular viability thus begins prior to the appearance of the strong blue fluorescence. This suggests that the UV light-induced CO release from **15** effectively initiates cell death.

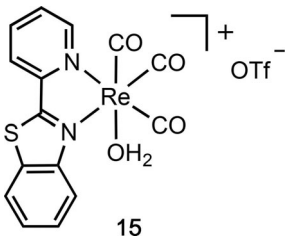

15

Figure 13. Structure of $[Re(H_2O)(CO)_3(pbt)]O_3SCF_3$.

2.5 Summary Comments

The luminescent metal carbonyl CO-releasing molecules reported to date are all photoCORMs based on the $[MX(CO)_3(\alpha\text{-diimine})]$ formulation with M=Re(I) or Mn(I). As can be noted from the summary shown in Figure 14, they cover an impressive range of emission wavelengths. There are four major ways to visualize photoCORM location and CO release using these complexes: (1) tracking of the photoCORM with no change in emission upon CO release; and (2) turn-off, (3) turn-on, and (4) two-tone luminescence change upon CO release. Challenges in the application of these photoCORMs for biological studies include the need for UV light to trigger CO release and the possible bioactivity of metal-containing by-products. Nevertheless, these metal-carbonyl photoCORMs exhibit high spatiotemporal control over CO delivery and offer the possibility of tracking CO release in cellular environments.

© 2019 Wiley-VCH Verlag GmbH & Co. KGaA, Weinheim

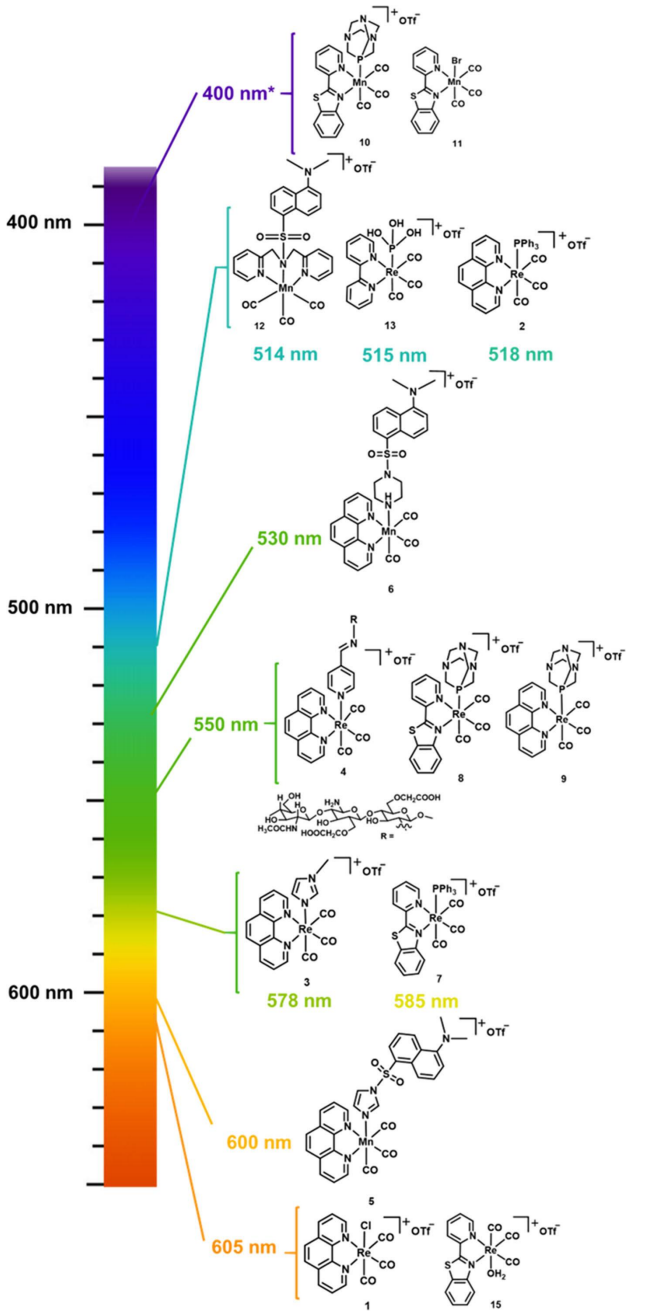

Figure 14. Summary of trackable metal carbonyl-based photoCORMs by their emission wavelengths. Note that those indicated by * involve emission of the free heterocyclic ligand following CO release.

3. Fluorescence Trackable Metal-Free CO-Releasing Molecules or their CO Release By-Products

Metal-free CORMs and photoCORMs have been recently developed that exhibit fluorescence trackability either before or following CO release. Organic CO-releasing molecules that can be followed via their fluorescence properties can be tracked prior to undergoing carbon-carbon bond cleavage to release CO. Metal-free compounds in the fluorescence turn-on category form new fluorescent polyaromatic by-products via the CO release reaction.

3.1 Potentially Trackable Fluorescein- and BODIPY-Based PhotoCORMs

The fluorescein analog 6-hydroxy-3-oxo-3*H*-xanthene-9-carboxylic acid (**16**, Figure 15) has been studied as an organic photoCORM in water.[14e] This compound exhibits a strong emission at ~530 nm with $\Phi_{em} = 0.39$ in methanol. Upon illumination at 500 nm, **16** releases CO from the carboxyl moiety via a proposed α-lactone intermediate. The product is stated to have a distinct emission signal but no data were provided. Studies of cellular uptake and distribution of **16** were not explored. It is possible that this photoCORM will have poor cellular uptake due to its overall negative charge at physiological pH. Typically, negatively charged fluorescein analogues lack cell-membrane permeability.[28] An additional complicating factor for the use of **16** in biological environments is its low CO release quantum yield ($\Phi \sim 7 \times 10^{-4}$) thus necessitating long exposure time to visible light. Studies involving 16 are also complicated by its low yield photochemical synthesis.

Klán and co-workers subsequently designed the *meso*-carboxy BODIPY derivatives **17a** and **17b** (Figure 16) as metal-free photoCORMs for possible biological applications.[14c] At pH = 7.4 in PBS buffer, **17a** has an absorbance maximum at 502 nm and exhibits a bright fluorescence emission at ~570 nm ($\Phi_{em} = 67\%$). Similar to **16**, illumination

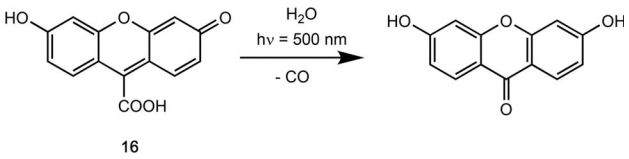

16

Figure 15. Visible light-induced CO release reactivity of **16**.

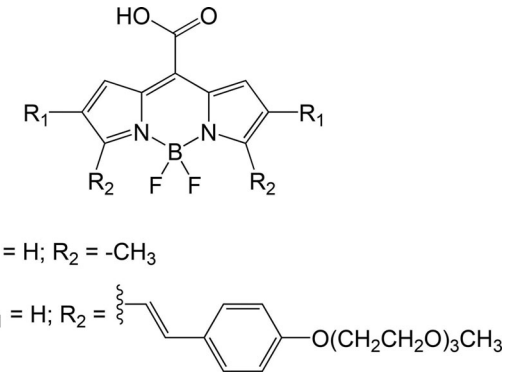

Figure 16. BODIPY-based photoCORMs **17a** and **17b**.

© 2019 Wiley-VCH Verlag GmbH & Co. KGaA, Weinheim

with visible light (~500 nm) results in CO release (87% yield anaerobic; 44% aerobic) and the formation of organic by-products that only absorb in the UV region. HRMS analysis of the product mixture showed the presence of 2-methylpyrrole and 2*H*-pyrrole-4-carbaldehyde, two common photochemical degradation products of other BODIPY derivatives.[29] It should be noted that while the reaction quantum yield for CO release from **17a** under anaerobic ($\Phi = 2.7 \pm 0.4 \times 10^{-4}$) and aerobic conditions ($\Phi = 1.1 \pm 0.1 \times 10^{-4}$) are low, the uncaging cross sections ($\varepsilon_{max}\Phi_{max}$) are high ($> 4 \times 10^5$). Compound **17b** (Figure 16) is a π-extended chromophore that exhibits an absorption maximum at ~650 nm with a tail to ~750 nm which is in the phototherapeutic (or tissue transparent) window. Illumination into either of the major absorption bands (368, 652 nm) or near the absorption tail at 732 nm results in CO release (91% yield) and the formation of a by-product that appears to contain a BODIPY chromophore. Neither **17a** and **17b** nor their photoproducts displayed toxicity in hepatoblastoma HepG2 and neuroblastoma SHSY-5Y cell lines up to a concentration of 100 μM.

To date, compounds **17a** and **17b** have not been used in cellular microscopy studies. Literature precedent with structurally similar BODIPY fluorophores that possess anionic carboxylate and oligo(ethylene glycol) ether groups has indicated that these compounds do not typically penetrate cell membranes.[30] Such membrane impermeability was attributed to the mismatch between the hydrophobicity and hydrophilicity in compound design impacting their interaction with the cell membrane components. Further studies of cellular uptake and distribution are needed for these *meso*-carboxy BODIPY derivatives to fully understand their delivery properties as CO donors. However, it is important to note that **17b** was demonstrated to deliver CO in vivo in studies involving nude SKH1 mice.

3.2 Turn-Off PhotoCORMs Based on the 3-Hydroxyflavone and 3-Hydroxyquinolone Motifs

In the pursuit of a trackable, biocompatible organic photoCORM, we have initiated investigations of bioinspired molecules having an extended 3-hydroxyflavone motif (**18**, Figure 17).[14d] This novel framework exhibits several advantageous features for the delivery of CO in biological environments. These include: (1) a clean, quantitative visible light-driven CO release reaction that occurs in both protic and hydrophobic environments, and under atmospheric levels of O_2 (18%) and hypoxic (1% O_2) conditions;[31,32] (2) green fluorescence prior to CO release (Figure 18) that enables monitoring of cellular uptake and distribution prior to CO release; and (3) a well-defined, non-toxic and non-emissive organic by-product (19, Figure 17). Recently, **18** was also shown to undergo CO release using two-photon excitation.[33] With regard to its luminescence properties, when excited at 410 nm, **18** exhibits two emission features at ~475 and ~580 nm that are associated with the normal (N*) and

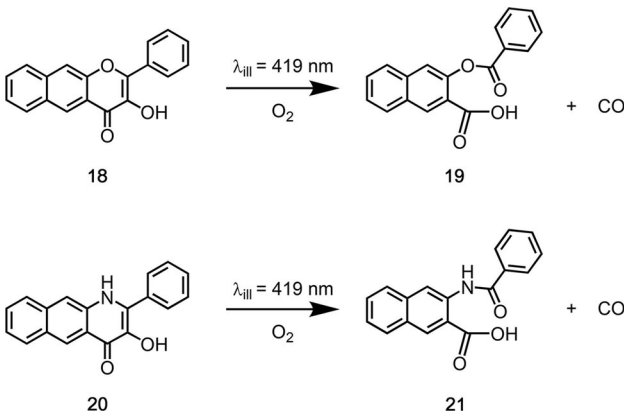

Figure 17. 3-hydroxyflavone and 3-hydroxyquinolone photoCORMs and their CO release reactivity.

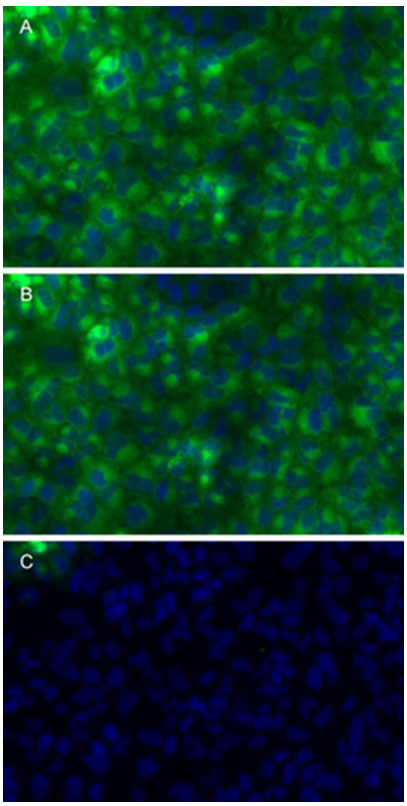

Figure 18. Fluorescence microscope images of human lung adenocarcinoma cells (A549 cells) treated with **18** for one hour. The images were collected after 30 s (A), 3 min (B), and 10 min (C) of exposure to a visible light LED source. The images represent overlay of the fluorescence detection of **18** (green) and the nuclear Hoechst 33342 stain (blue). Loss of fluorescence with increasing length of exposure to visible light is consistent with photoinduced CO release from **18**. Reprinted from (S. N. Anderson, J. M. Richards, H. J. Esquer, A. D. Benninghoff, L. M. Berreau, *ChemistryOpen* **2015**, *4*, 590–594.)

© 2019 Wiley-VCH Verlag GmbH & Co. KGaA, Weinheim

tautomeric (T*) excited state forms, respectively. The ~580 nm emission can be easily monitored using the GFP channel settings on a fluorescence microscope (Figure 18). Cell-based studies using **18** have shown good cellular uptake, with the compound being successfully visualized in the cytosol of human lung adenocarcinoma cells (A549 cells) and human umbilical vein cells (HUVECs).[14d,34] Compound **18** exhibits minimal or no toxicity in both cell lines and the CO release by-product **19** is non-toxic up to 100 μM.

The 3-hydroxyquinolone photoCORM **20** (Figure 17) exhibits many properties similar to its flavone analog **18**, including quantitative, visible-light induced CO release followed by fluorescence turn-off that can be detected using the GFP channel.[14b] Notably, **20** is best delivered to cells using bovine serum albumin (BSA) as a carrier protein. The binding constant for **20** to BSA is more than >900-fold stronger than that of **19**, with both binding to the protein in a 1 : 1 stoichiometry.[14b,31] In the absence of visible light and in the presence of a physiologically relevant amount of BSA (0.6 mM) **20** exhibits no toxicity up to 100 μM in A549 cells whereas **19** is mildly toxic (IC_{50} = 82 μM). Upon illumination with visible light (419 nm) **20** produces greater CO-induced toxicity than **19** (IC_{50} = 24 μM and 96 μM, respectively). This difference may result from variances in protein binding and/or cellular uptake. It is worth noting that **20** is the first photoCORM to show nanomolar anti-inflammatory effects.[14b] The CO release byproduct **21** is non-toxic up to 100 μM.

Recently Soboleva, *et al.* have demonstrated that the fluorescence properties of the 3-hydroxyflavone framework can be applied for tracking a mitochondria-targeted phosphonium-appended analog.[34] As shown in Figure 19, co-localization of **22** with MitoTracker Red (MTR) is evident via confocal microscopy using A549 cells. The localization of this compound to mitochondria enabled a comparative evaluation of the effect of triggered CO release from cytosolic **18** versus mitochondria-targeted **22** on mitochondrial bioenergetics. It was found that at a concentration of 10 μM release of CO from the two photoCORMs produced similar effects in terms of decreasing basal respiration, ATP production, maximal respiration, and the reserve capacity of A549 cells. This result suggests that localized subcellular delivery of CO may not be needed to achieve effects due to the inertness and diffusability of CO.

The 3-hydroxyflavone and 3-hydroxyquinolone photoCORM motifs are easily modified structures that can be customized for a variety of applications involving trackable CO delivery. These include sense and release applications wherein the CO-releasing 3-OH unit in **18** is unmasked for CO release only in the presence of a specific bioanalyte.[32,33,35]

3.3 Turn-On CO Donors Based on the Release of a Fluorescent By-Product

Similar to the turn-on metal carbonyl compounds described herein, organic CORMs in which the CO release reaction

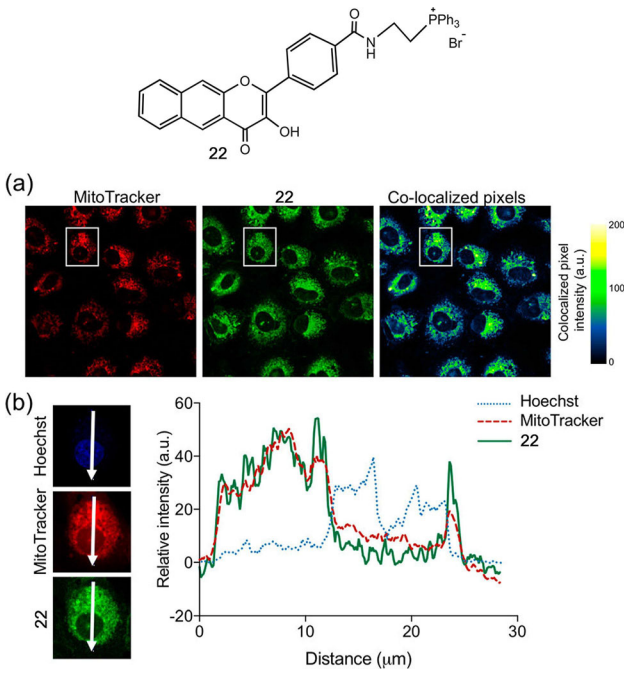

Figure 19. (top) Structure of a mitochondria-targeted flavonol-based photoCORM. (bottom) Confocal images of A549 cells co-stained with **22**, MitoTracker Red (MTR), and Hoechst 33342. (a) Independent and co-localized pixels of **22** and MTR. (b) Overlaid intensity profile of regions of interest (ROIs) in the co-stained A549 cells as indicated by the white arrows. Reprinted (adapted) with permission from (T. Soboleva, H. J. Esquer, S. N. Anderson, L. M. Berreau, A. D. Benninghoff, *ACS Chem. Biol* **2018**, *13*, 2220–2228). Copyright (2018) American Chemical Society.

results in the formation of a trackable organic fluorophore have been developed. The two scaffolds reported to date that exhibit this chemistry involve the formation of fluoranthene- and anthracene-type derivatives. In the following sections we discuss the CORMs built to produce these fluorescent by-products upon CO release and the feasibility of tracking each type of compound in living cells.

3.3.1 Click and Release CORMs: Intra- and Inter-Molecular Inverse Electron Demand Diels-Alder (DA_{inv}) CO-Releasing Reactions Tracked via the Blue Emission of a Fluoranthene-Based By-Product

Wang and co-workers have explored the development of organic prodrugs that undergo cheletropic reaction under physiologically relevant conditions to spontaneously release CO.[13,36–38] These generally non-toxic molecules (up to 100 μM) are designed to undergo inter- or intra-molecular inverse electron demand Diels-Alder (DA_{inv}) reactions with tunable CO release rates. The unimolecular CO prodrugs (Figure 20) all undergo spontaneous CO release to produce fluorescent fluoranthene-containing products that can be tracked in cellular studies. While not commonly used as a dye

© 2019 Wiley-VCH Verlag GmbH & Co. KGaA, Weinheim

Israel Journal of Chemistry

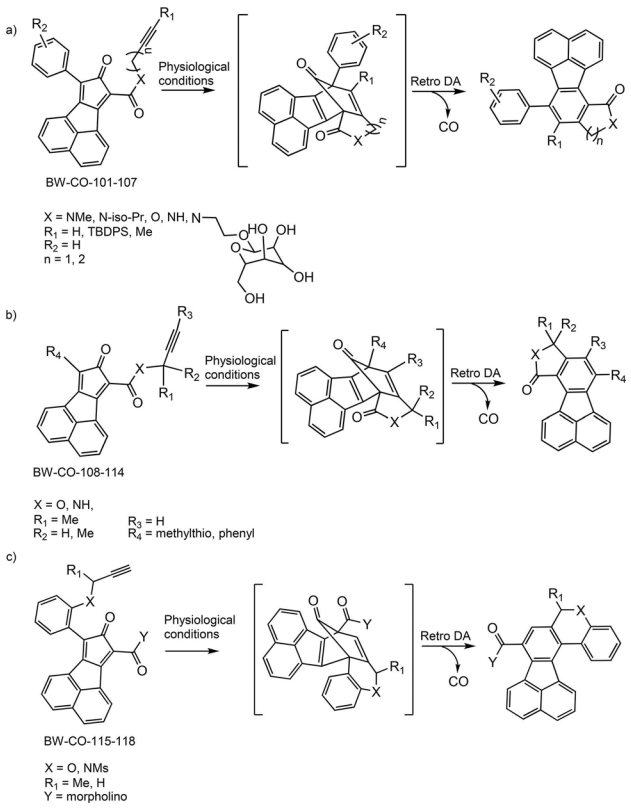

Figure 20. Examples of intramolecular inverse electron demand DA_{inv} reactions leading to CO release and the formation of a trackable fluoranthene-containing by-product.

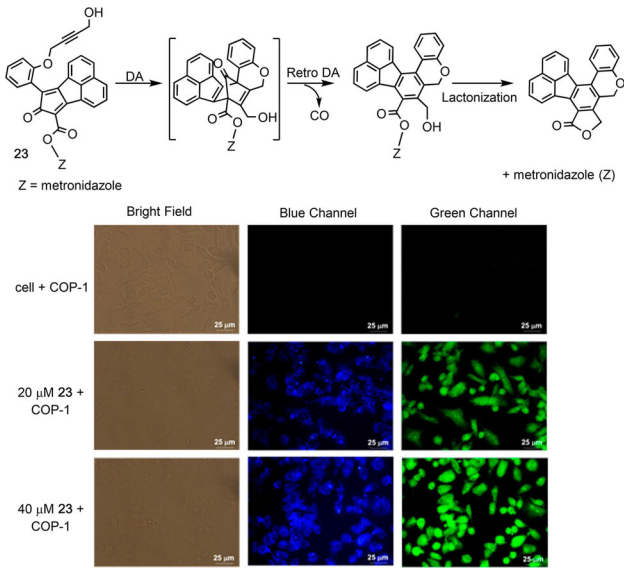

Figure 21. (top) Cascade delivery system for CO and metronidazole with release of fluorescent by-product. (bottom) Concentration-dependent increase in fluorescence intensity of the fluoranthene-based by-product (blue channel) and COP-1 CO detection probe (green channel) after 6 h incubation of prodrug **23**. Reprinted (adapted) with permission from (L. K. C. De La Cruz, S. L. Benoit, Z. Pan, B. Yu, M. J. Maier, X. Ji, B. Wang, *Org. Lett.* **2018**, *20*, 897–900). Copyright (2018) American Chemical Society.

for cellular assays, fluoranthene and its derivatives have absorption and emission features suitable for cellular imaging, with $\lambda_{ex} \sim 370$ nm and $\lambda_{em} \sim 460$ nm in DMSO/PBS (5 : 1, pH 7.4) and a reported fluorescence quantum yield in water of 0.23 ± 0.02.[39] While discussion of the kinetics of CO release from the compounds shown in Figure 20 is outside the scope of this review, the formation of the fluoranthene product in each reaction type enables real-time fluorescence monitoring of CO release in DMSO/PBS (4 : 1, pH 7.4) at 37 °C.

In terms of cellular studies, the emission features of fluoranthene can easily be followed using the DAPI channel settings in a regular fluorescence microscope. BW-CO-103 was the first compound of this type to be examined with regard to the visualization of CO delivery in cells.[13b] Imaging of RAW 264.7 cells revealed a dose- and time-dependent increase in cytosolic fluorescence intensity for the fluoranthene-containing by-product. Production of CO under these conditions was also shown via use of the COP-1 fluorescent CO sensor.[24] The derivatives BW-CO-109 and BW-CO-117 were subsequently shown to exhibit a concentration-dependent increase in fluorescence intensity for CO delivery in RAW 264.7 cells.[36] A cascade drug delivery system (**23**, Figure 21) has also been developed on this premise wherein a drug payload (metronidazole) is released along with CO and a fluoranthene by-product. The latter provides visual evidence of the release of all three molecules.[37]

The Wang group has also ingeniously applied the ability to visualize CO delivery in a bimolecular approach in targeting complementary reaction components to mitochondria in vitro and in vivo (**24** and **25**, Figure 22).[38] The subcellular co-localization of both molecules was used to enhance the concentration and probability of collision between the two

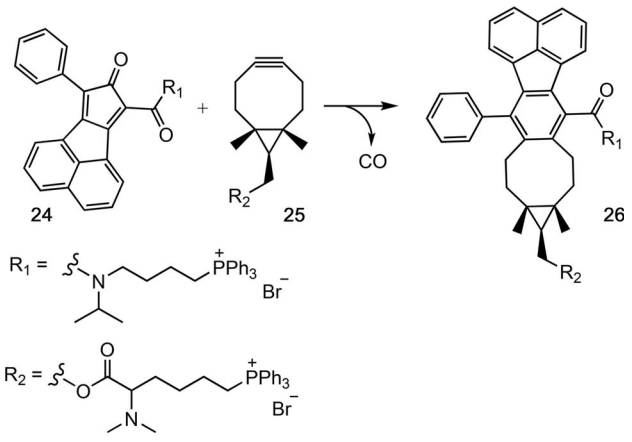

Figure 22. Intermolecular inverse electron demand DA_{inv} reaction based CO-releasing molecules targeted for reactivity at mitochondria.

© 2019 Wiley-VCH Verlag GmbH & Co. KGaA, Weinheim

reactive species leading to CO release. Fluorescence imaging demonstrated that the blue emissive CO release by-product **26** co-localizes with the mitochondria-specific dye MitoTracker Deep Red in RAW 264.7 cells. This implies that the reaction between **24** and **25** leading to CO and fluorophore release does occur at mitochondria. However, no effects of CO on mitochondrial function were reported.

3.3.2 Unsaturated α-Diketones (α-DKs): Visible-Light Induced CO-Releasing Molecules Tracked via the Blue Emission of Anthracene-Based By-Products

Unsaturated cyclic α-diketones (**27**–**29**, Figure 23) containing a carbonyl bridge across the 9 and 10 positions of the anthracene, are known to undergo photo-decarbonylation to release CO in non-aqueous environments.[14f] Illumination with visible light leads to cleavage of the α-diketone bridge with the release of two molecules of CO and regeneration of anthracene or anthracene analogues, which are blue emissive molecules. A challenge with using these α-diketones in aqueous environments is the rapid hydration of the carbonyl moieties. This limits the usability of these compounds to encapsulated forms for applications in biological systems.[14f] Liao and co-workers synthesized and characterized micelle-encapsulated α-diketones of **27**–**29** exploring their intracellular visible light-induced (λ_{ill} = 470 nm) activation and CO release in acute myeloid leukemia cells (KG1 cells).[14f] The released anthracene-based by-product fluorophore from micelle-encapsulated **29** could easily be visualized using the standard DAPI channel settings of a fluorescence microscope due to a relatively high fluorescence quantum yield of anthracene (0.31 ± 0.02 in water).[39] Cell viability tests performed over 72 h showed no change in viability of cells exposed to the micelle form of **29** or visible light.

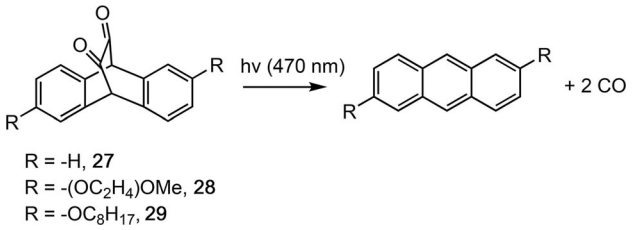

Figure 23. Visible light-induced α-diketone reactivity resulting in the release of anthracene-based fluorophores and CO.

Notably, the α-diketone-type photoCORM **27** has been incorporated into a biodegradable polycaprolactone material to fabricate fibrous scaffolds used for cardiovascular tissue engineering.[40] The loaded, electrospun poly(ε-caprolactone) scaffolds can be photoactivated to release CO in both anhydrous and cell culture conditions. Similar to the free molecules, the CO release from this material was conveniently monitored via the development of blue fluorescence emission from the anthracene-based by-product generated in the process of CO delivery.

3.4 Summary Comments

Tracking of CO delivery from organic CORMs and photoCORMs is currently possible via two approaches: monitoring of the fluorescence decay of the CO release donor itself, or by the release of a florescent by-product. Importantly, the turn-off organic photoCORMs enable visualization of the location of the molecule prior to CO release, thus providing direct evidence for an intracellular reaction. While tracking of a reporter fluorophore resulting from a CO release reaction is also convenient, it may not be a definitive indicator of the location of CO release. For example, it is possible that the CO release reaction occurs extracellularly with subsequent diffusion of CO and uptake of the fluorophore by-product into cells.

4. Outlook

Development of novel CO-releasing molecules is an active area of research directed at producing potential therapeutics and new molecular tools to gain a better understanding of the reactivity of CO in biology. Visualizing the site of CO delivery in cells is an important current goal for more accurate spatiotemporal control. In this review, we have summarized the molecular structures reported to date that enable luminescence tracking related to CO delivery. We have discussed the strengths and weaknesses of these systems in order to define features that may be advantageous in the design of the next generation of trackable CORMs and photoCORMs. In terms of specific goals, in our opinion, the field will be advanced by the further development of luminescent CO-releasing molecules that: (1) enable visualization of cellular uptake of the compound and the CO release event via distinct luminescence signals (two-tone tracking); (2) are well-defined in terms of their reaction by-products; and (3) involve non-toxic components. The scaffolds discussed herein are likely to inspire the development of new structures to address this goal and others in this exciting field.

Acknowledgements

We thank the NIH (R15GM124596 to L.M.B), the American Heart Association (18PRE34030099; predoctoral fellowship to T.S.) and the USU Office of Research and Graduate Studies (PDRF fellowship to T.S.) for financial support.

© 2019 Wiley-VCH Verlag GmbH & Co. KGaA, Weinheim

References

[1] a) D. Wu, A. C. Sedgwick, T. Gunnlaugsson, E. U. Akkaya, J. Yoon, T. D. James, *Chem. Soc. Rev.* **2017**, *46*, 7105–7123; b) J. Yan, S. Lee, A. Zhang, J. Yoon, *Chem. Soc. Rev.* **2018**, *47*, 6900–6916; c) Y. L. Pak, K. M. K. Swamy, J. Yoon, *Sensors* **2015**, *15*, 24374–24396.

[2] a) R. Tenhunen, H. S. Marver, R. Schmid, *Proc. Natl. Acad. Sci. USA* **1968**, *61*, 748–755; b) R. Tenhunen, H. S. Marver, R. Schmid, *J. Biol. Chem.* **1969**, *244*, 6388–6394; c) L. E. Otterbein, A. M. Choi, *Am. J. Physiol. Lung Cell. Mol. Physiol.* **2000**, *279*, L1029-1037.

[3] A. A. Untereiner, L. Wu, R. Wang, in *Gasotransmitters:Physiology and Pathophysiology*, (Eds.: A. Hermann, G. F. Sitdikova, T. M. Weiger), Springer-Verlag: Berlin Heidelberg **2012**, p. 37–70.

[4] R. Motterlini, L. E. Otterbein, *Nat. Rev. Drug Discovery* **2010**, *9*, 728–743.

[5] R. Motterlini, R. Foresti, *Am. J. Physiol. Cell Physiol.* **2017**, *312*, C302-C313.

[6] R. Motterlini, B. E. Mann, R. Foresti, *Expert Opin. Invest. Drugs* **2005**, *14*, 1305–1318.

[7] B. E. Mann, *Top. Organomet. Chem.* **2010**, *32*, 247–285.

[8] R. Motterlini, J. E. Clark, R. Foresti, P. Sarathchandra, B. E. Mann, C. J. Green, *Circ. Res.* **2002**, *8*, E17-24.

[9] R. Foresti, J. Hammad, J. E. Clark, T. R. Johnson, B. E. Mann, A. Friebe, C. J. Green, R. Motterlini, *Br. J. Pharmacol.* **2004**, *142*, 453–460.

[10] S. H. Crook, B. E. Mann, A. J. H. M. Meijer, H. Adams, P. Sawle, D. Scapens, R. Motterlini, *Dalton Trans.* **2011**, *40*, 4230–4235.

[11] a) E. Kottelat, F. Zobi, *Inorganics* **2017**, *5*, 24; b) M. A. Wright, J. A. Wright *Dalton Trans.* **2016**, *45*, 6801–6811; c) U. Schatzschneider, *Br. J. Pharmacol.* **2015**, *172*, 1638–1650; d) I. Chakraborty, S. J. Carrington, P. K. Mascharak, *Acc. Chem. Res.* **2014**, *47*, 2603–2611; e) M. A. Gonzales, P. K. Mascharak, *J. Inorg. Biochem.* **2014**, *133*, 127–135. f) C. C. Romão, W. A. Blättler, J. D. Seixas, G. J. L. Bernardes, *Chem. Soc. Rev.* **2012**, *41*, 3571–3583; g) U. Schatzschneider, *Inorg. Chim. Acta* **2011**, *374*, 19–23.

[12] A. C. Kautz, P. C. Kunz, C. Janiak, *Dalton Trans.* **2016**, *45*, 18045–18063.

[13] a) X. Ji, B. Wang, *Acc. Chem. Res.* **2018**, *51*, 1377–1385; b) X. Ji, C. Zhou, K. Ji, R. E. Aghoghovbia, Z. Pan, V. Chittavong, B. Ke, B. Wang, *Angew. Chem. Int. Ed. Engl.* **2016**, *55*, 15846–15851.

[14] a) T. Slanina, P. Šebej, *Photochem. Photobiol. Sci.* **2018**, *17*, 692–710; b) M. Popova, T. Soboleva, S. Ayad, A. D. Benninghoff, L. M. Berreau, *J. Am. Chem. Soc.* **2018**, *140*, 9721–9729; c) E. Palao, T. Slanina, L. Muchová, T. Šolomek, L. Vitek, P. Klán, *J. Am. Chem. Soc.* **2016**, *138*, 126–133; d) S. N. Anderson, J. M. Richards, H. J. Esquer, A. D. Benninghoff, A. M. Arif, L. M. Berreau, *ChemistryOpen* **2015**, *4*, 590–594; e) L. A. P. Antony, T. Slanina, P. Šebej, T. Šolomek, P. Klán, *Org. Lett.* **2013**, *15*, 4552–4555. f) P. Peng, C. Wang, Z. Shi, V. K. Johns, L. Ma, J. Oyer, A. Copik, R. Igarashi, Y. Liao, *Org. Biomol. Chem.* **2013**, *11*, 6671–6674.

[15] E. A. Specht, E. Braselmann, A. E. Palmer, *Annu. Rev. Physiol.* **2017**, *79*, 93–117.

[16] R. A. Karigan, B. P. Sullivan, D. P. Rillema, *Top. Curr. Chem.* **2007**, *281*, 45–100.

[17] a) I. Chakraborty, J. Jimenez, W. M. C. Sameera, M. Kato, P. K. Mascharak, *Inorg. Chem.* **2017**, *56*, 2863–2873; b) I. Chakraborty, J. Jimenez, P. K. Mascharak, *Chem. Commun.* **2017**, *53*, 5519–5522.

[18] J. Jimenez, M. N. Pinto, J. Martinez-Gonzalez, P. K. Mascharak, *Inorg. Chim. Acta* **2019**, *485*, 112–117.

[19] J. Jimenez, I. Chakraborty, A. Dominguez, J. Martinez-Gonzalez, W. M. C. Sameera, P. K. Mascharak, *Inorg. Chem.* **2018**, *57*, 1766–1773.

[20] U. Reddy, G. J. Axthelm, P. Hoffmann, N. Taye, S. Gläser, H. Görls, S. L. Hopkins, W. Plass, U. Neugebauer, S. Bonnet, A. Schiller, *J. Am. Chem. Soc.* **2017**, *139*, 4991–4994.

[21] I. Chakraborty, S. J. Carrington, J. Hauser, S. R. J. Oliver, P. K. Mascharak, *Chem. Mater.* **2015**, *27*, 8387–8397.

[22] I. Chakraborty, S. J. Carrington, G. Roseman, P. K. Mascharak, *Inorg. Chem.* **2017**, *56*, 1534–1545.

[23] S. J. Carrington, I. Chakraborty, J. M. L. Bernard, P. K. Mascharak, *ACS Med. Chem. Lett.* **2014**, *5*, 1324–1328.

[24] B. W. Michel, A. R. Lippert, C. J. Chang, *J. Am. Chem. Soc.* **2012**, *134*, 15668–15671.

[25] A. E. Pierri, A. Pallaoro, G. Wu, P. C. Ford, *J. Am. Chem. Soc.* **2012**, *134*, 18197–18200.

[26] a) H. Hori, K. Koike, M. Ishizuka, K. Takeuchi, T. Ibusuki, O. Ishitani, *J. Organomet. Chem.* **1997**, *530*, 169–176; b) K. Koike, N. Okoshi, H. Hori, K. Takeuchi, O. Ishitani, H. Tsubaki, I .P. Clark, M. W. George, F. P. A. Johnson, J. J. Turner, *J. Am. Chem. Soc.* **2002**, *124*, 11448–11455.

[27] S. J. Carrington, I. Chakraborty, J. M. L. Bernard, P. K. Mascharak, *Inorg. Chem.* **2016**, *55*, 7852–7858.

[28] T. Kowada, H. Maeda, K. Kikuchi, *Chem. Soc. Rev.* **2015**, *44*, 4953–4972.

[29] S. Mula, A. K. Ray, M. Banerjee, T. Chaudhuri, K. Dasgupta, S. Chattopadhyay, *J. Org. Chem.* **2008**, *73*, 2146–2154.

[30] Y. Ni, L. Zeng, N.-Y. Kang, K.-W. Huang, L. Wang, Z. Zeng, Y.-T. Chang, J. Wu, *Chem. Eur. J.* **2014**, *20*, 2301–2310.

[31] M. Popova, T. Soboleva, A. M. Arif, L M. Berreau, *RSC Adv.* **2017**, *7*, 21997–22007.

[32] T. Soboleva, H. J. Esquer, A. D. Benninghoff, L. M. Berreau, *J. Am. Chem. Soc.* **2017**, *139*, 9435–9438.

[33] Y. Li, Y. Shu, M. Liang, X. Xie, X. Jiao, X. Wang, B. Tang, *Angew. Chem. Int. Ed.* **2018**, *57*, 12415–12419.

[34] T. Soboleva, H. J. Esquer, S. N. Anderson, L. M. Berreau, A. D. Benninghoff, *ACS Chem. Biol.* **2018**, *13*, 2220–2228.

[35] T. Soboleva, A. D. Benninghoff, L. M. Berreau, *ChemPlusChem* **2017**, *82*, 1408–1412.

[36] Z. Pan, V. Chittavong, W. Li, J. Zhang, K. Ji, M. Zhu, X. Ji, B. Wang, *Chem. Eur. J.* **2017**, *23*, 9838–9845.

[37] L. K. C. De La Cruz, S. L. Benoit, Z. Pan, B. Yu, R. J. Maier, X. Ji, B. Wang, *Org. Lett.* **2018**, *20*, 897–900.

[38] Y. Zheng, X. Ji, B. Yu, K. Ji, D. Gallo, E. Csizmadia, M. Zhu, M. R. Choudhury, L. K. C. De La Cruz, V. Chittavong, Z. Pan, Z. Yuan, L. E. Otterbein, B. Wang, *Nat. Chem.* **2018**, *10*, 787–794.

[39] F. P. Schwarz, S. P. Wasik, *Anal. Chem.* **1976**, *48*, 524–528.

[40] E. Michael, N. Abeyrathna, A. V. Patel, Y. Liao, C. A. Bashur, *Biomed. Mater.* **2016**, *11*, 025009.

Manuscript received: December 1, 2018
Revised manuscript received: January 13, 2019
Version of record online: February 11, 2019

© 2019 Wiley-VCH Verlag GmbH & Co. KGaA, Weinheim